Pramāṇa – J. Phys., Vol. 27, Nos 1 & 2, July & August 1986, pp. 139–160.
© Printed in India.

Proton-nucleus optical model potential at low energies—a review

M K MEHTA and S KAILAS
Nuclear Physics Division, Bhabha Atomic Research Centre, Bombay 400 085, India

Abstract. Ever since it was proposed more than three decades ago, the nuclear optical model has been very successful in interpreting a large body of nucleon-induced nuclear reaction data in terms of a complex nucleon-nucleus potential. Rapid progress both in the experimental measurements and the theoretical developments in the last two decades has led to a better understanding of this nucleon-nucleus optical potential. From the parameter-fitting phenomenological stage, the optical model has come a long way and it is now possible to calculate the nucleon-nucleus optical potential in a reasonable way starting from the fundamental nucleon-nucleon interaction. Excellent reviews on various aspects of the optical model exist in the literature for proton energies above 10 MeV. The present article is an attempt to review comprehensively the status of the proton-nucleus optical potential at low proton energies, below the Coulomb-barrier, for target nuclei with mass numbers lying between 40 and 130. The sets of phenomenological optical potential derived mostly from (p, n) reaction data are reviewed and their applicabilities discussed. The neutron-nucleus optical model is referred to wherever it is relevant. Microscopic calculations for one case is carried out and compared with the corresponding phenomenological values.

Keywords. Low energy proton + nucleus optical model potential; phenomenological analysis; real and imaginary potential parameters.

PACS No. 24·10; 25·40

1. Introduction

Since its application by Feshbach *et al* (1954) to explain the extensive neutron-nucleus cross section data, the nuclear optical model has come of age and has been fully established as the most suitable and physical phenomenological model for the description of the nucleon-nucleus interaction. The concept has proved itself to be a very useful tool in parameterizing the interaction between the various projectiles, n, p, d, ^{3}He, ^{4}He, and the target nuclei (Hodgson 1971) and has become the basis on which reactions between complex nuclei are also analyzed and interpreted (Satchler and Love 1979). The phenomenological parametrization of the nucleon-nucleus interaction through optical model is also considered to be an important intermediate step towards full microscopic understanding of this interaction. In this model the nucleon-nucleus interaction is parametrized in terms of a complex potential, $V(r)$, which has a Woods-Saxon form for the real part and a Woods-Saxon or derivative Woods-Saxon form for the imaginary part (Hodgson 1971). Over the years considerable progress has been made both in the microscopic and the phenomenological aspects of the nucleon-nucleus optical model (Hodgson 1984, 1985; Rapaport 1982; Schwandt 1983; Von Geramb 1979, 1985). We are

The authors felicitate Prof. D S Kothari on his eightieth birthday and dedicate this paper to him on this occasion.

now in a position to write down the nucleon-nucleus optical potential with reasonable accuracy given the mass number and the atomic number of the nucleus, the nucleon type and the energy. From systematic phenomenological analyses, Perey (1963) obtained the optical model parameters for protons with energies (E_p) lying between 9 and 22 MeV and for target mass numbers (A_T) between 30 and 100. While Becchetti and Greenlees (1969) determined them for E_p = 10–50 MeV, Menet *et al* (1971) obtained them for E_p = 30–60 MeV. For protons at higher energies upto 200 MeV, Schwandt (1983) determined them. For neutrons the status of the optical potential is reviewed by several workers (Rapaport 1982; Hodgson 1984; Walter and Guss 1985; Smith *et al* 1986).

Low energy neutron-nucleus optical model is very well studied and reviews have been written on this topic (Rapaport 1982; Hodgson 1984; Smith *et al* 1986). But this is not the case for the low energy proton-nucleus optical model. The present work is aimed at reviewing the experimental and theoretical work regarding the proton-nucleus interaction in the scheme of the nuclear optical model at low energies. We are particularly concerned with the optical potential for proton energies which are conventionally defined as sub-Coulomb i.e. below the Coulomb barrier for the proton-target system, which varies from 6·5 MeV for ^{45}Sc to 11·4 MeV ^{130}Te (figure 1). There are several groups the world over who contributed actively in the last decade in generating data useful for determining the proton optical potential at sub-Coulomb energies (Oak Ridge, U.S.A.—Johnson *et al* 1979; Trombay, India—Kailas and Mehta 1982; Erlangen, FRG—Finckh 1980; Melbourne, Australia—Sargood 1982; Kentucky, U.S.A.—Flynn *et al* 1985; California, U.S.A.—Esat *et al* 1981).

The optical potential at this low energy sub-Coulomb region is interesting from several points of view:

(i) This energy region more or less connects the negative energy bound states with the positive energy unbound states and hence the data in this region provide a handle to understand this transition region (Mahaux and Ngo 1981; Bauer *et al* 1982; Finlay *et al* 1985).

(ii) The presence of the single particle/size resonances can be seen more clearly in this low energy region (Johnson *et al* 1977a). It turns out that at these sub-Coulomb energies, the Coulomb barrier, by virtue of its height relative to the spreading width from the absorptive potential, can quasibind a single-particle state. In view of this it is

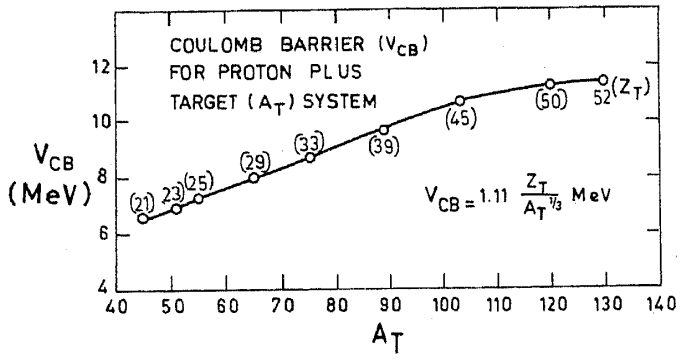

Figure 1. Coulomb barrier V_{cB} plotted as a function of the target mass number A_T. $V_{cB} = Z_T e^2/R$ with e^2 = 1·44 and R = 1·3 $A_T^{1/3}$ (fm).

more likely that a single particle resonance will be sharpened sufficiently to be observed as a function of proton energy for a given nucleus.

(iii) In determining the optical model parameters, effects due to nuclear structure—level density, collective and shell effects—are seen rather strongly in this energy region (Grimes 1980; Hodgson 1985; Johnson *et al* 1977b; Kailas *et al* 1979; Flynn *et al* 1985).

(iv) Using the proton optical parameters determined in this energy region, the cross-sections at lower energies which are of interest to astrophysics and for other applications can be calculated.

(v) The nucleus-nucleus potential at low energies can be determined from a knowledge of nucleon-nucleus potential at these energies and by employing "folding model techniques".

(vi) In performing DWBA calculations for transfer reactions and inelastic scattering involving protons at these energies the proton-nucleus optical potentials are used. Even in certain special reactions like (n, p), the proton-nucleus optical potentials are used. (Avrigeanu *et al* 1986)

(vii) The energy variation of the imaginary part of the optical potential has an effect on the real part manifested through the dispersion relation (Mahaux *et al* 1986). This effect is most pronounced at energies close to the Fermi and sub-Coulomb energies.

In the present work, we have reviewed this field and summarized the various features of the proton-nucleus optical potential for $E_p \sim 1$–7 MeV and for target nuclei with $A_T \sim 40$–130. Both the phenomenological and the microscopic models used in the analysis are discussed. Wherever possible the connection to the neutron-nucleus optical model has been brought out. A brief discussion of the experimental techniques employed in measuring the proton scattering and absorption data is given in §2. The determination of the proton optical model parameters—the methodology, the salient features and the systematics of the parameters—forms the subject matter of §3. In §4 we discuss the strength function and the effective mass concepts as applied to the present work. The microscopic and the phenomenological models are also compared here. Section 5 sets out the conclusions.

2. Experimental techniques

When proton collides with the target nucleus at low energies, broadly speaking there are two processes that take place, the elastic scattering (σ_{el}) and the absorption (σ_{abs}) followed by various reactions leading to emission of not only protons but gamma rays, neutrons, alpha and other particles. The optical parameters are generally determined by measurement and analysis of σ_{el} and σ_{abs}. Determination of σ_{el} involves measurement of angular distribution and also excitation function at selected backward angles. Normally this is carried out in a scattering chamber using silicon surface barrier detectors. As explained in the next section, in the determination of the optical model parameters, at sub-Coulomb energies, there is greater sensitivity to σ_{abs} ($\approx \sigma_{p,n}$) than σ_{el} data.

At sub-Coulomb energies and at proton energies above the neutron threshold the neutron emission dominates over the other emission channels and hence $\sigma_{abs} \approx \sigma_{p,n}$. At low energies by measuring the (p, n) cross-section, the proton absorption cross-section can be determined conveniently without much error. Normally the excitation function of the (p, n) reaction is measured from the threshold to 5 or 7 MeV (high energy limit

dictated by the accelerator used for measurement) in convenient energy steps using either thick target to average over fine structures or thin target followed by energy averaging to simulate the thick target data. The targets employed have been either self-supporting foils or material deposited on suitable backing materials. The total (p, n) cross-sections have been measured using the activation technique when the residual nuclei are radioactive with suitable half-lives. The most widely used technique for (p, n) measurement involves use of either the long counter or the 4π geometry neutron counter. Because of easy portability the long counter has been usually preferred whenever angular distribution measurements are carried out. However, for the total cross-section measurements the 4π geometry counter is the most suitable as it integrates over all angles and sums over all neutron groups. It has a large efficiency (typical 5–10%) and has a fairly flat response for a range of neutron energies. In the literature several counters of this type—their design and efficiency details—have been reported (Macklin 1957; Macklin *et al* 1972; Sekharan 1966; Sekharan *et al* 1976; Gupta and Kerekatte 1971; Gabbard 1977). Generally, $\sigma_{p,n}$ measurements have errors of 5–10% consisting of uncertainties in efficiency and percentage number of the high energy neutrons (when the efficiency of the counter is not uniform enough with respect to energy) and in the target thickness. A very high degree of accuracy ($\sim 1\%$) in $\sigma_{(p,n)}$ measurements has been reported by Johnson *et al* (1977a) in special cases.

For proton energies below the neutron threshold the other reaction channel viz (p, γ), (p, p') will become increasingly important. In the present discussion we will be concerned mainly at proton energies above the neutron threshold. Hence the basic measurements of interest are σ_{el} and $\sigma_{p,n}$. In the present article, most of the relevant (p, n) reactions studied, have been reviewed regarding their interpretation in terms of the optical model, and are listed in table 1. For further details of experimental arrangements and measurements the reader may refer to the original articles listed in table 1.

3. Optical model

3.1 *General considerations*

The nuclear reactions in this low energy region are best described by the compound nuclear statistical model developed by Hauser and Feshbach (1952). Based on this formalism, the cross-section for the (p, n) reaction can be written as (Kailas *et al* 1975),

$$\sigma_{p,n} = \pi\lambda_p^2 \sum_{J_i, j_p, l_p} \frac{(2J_i+1)}{(2J_0+1)(2S_p+1)} \frac{T_{l_p j_p}(E_p) \sum_{l_n, j_n, E_n} T_{l_n j_n}(E_n)}{T_{l_p j_p}(E_p) + \sum_{l_n, j_n, E_n} T_{l_n j_n}(E_n)}$$

where J_0 and S_p equal the target and the projectile spins, T_p and T_n are the proton and the neutron transmission coefficients, J_i equals the compound nuclear spin. In writing the above we have assumed that the direct reaction contribution is negligible and have considered only the proton and the neutron emission probabilities. If we further make the assumption that

$$\sum T_{l_n j_n}(E_n) \gg T_{l_p j_p}(E_p),$$

Table 1. (p, n) data.

Target	$Q_{p,n}$ (MeV)	Reference	Target	$Q_{p,n}$ (MeV)	Reference
^{41}K	−1·210	Saini *et al* (1983)	^{93}Nb	−1·201	Johnson *et al* (1979)
^{45}Sc	−2·841	Iyengar (1967)	^{94}Zr	−1·704	Flynn *et al* (1979)
^{48}Ca	−0·493	Gulzar Singh *et al* (1982)	^{95}Mo	−2·441	Flynn *et al* (1979)
^{49}Ti	−1·384	Kennett *et al* (1980a)	^{96}Zr	−0·568	Flynn *et al* (1985)
^{50}Ti	−2·997	Kailas *et al* (1975)	^{98}Mo	−2·372	Flynn *et al* (1979)
		Kennett *et al* (1980b)	^{100}Mo	−1·118	Flynn *et al* (1985)
^{51}V	−1·534	Kailas *et al* (1985)	^{103}Rh	−1·337	Johnson *et al* (1979)
		Zyskind *et al* (1980)	^{105}Pd	−2·083	Johnson *et al* (1979)
^{53}Cr	−1·380	Johnson *et al* (1960)			
^{54}Cr	−2·161	Kailas *et al* (1975)	^{107}Ag	−2·199	Hershberger *et al* (1980)
^{55}Mn	−1·015	Viyogi *et al* (1978)	^{109}Ag	−0·951	Hershberger *et al* (1980)
^{57}Fe	−0·353	Johnson *et al* (1960)	^{110}Pd	−1·650	Johnson *et al* (1979)
^{59}Co	−1·855	Kailas *et al* (1975)	^{111}Cd	−1·869	Johnson *et al* (1979)
^{61}Ni	−3·018	Johnson *et al* (1960)	^{113}Cd	−0·485	Johnson *et al* (1979)
^{64}Ni	−2·461	Johnson *et al* (1960)	^{114}Cd	−2·215	Johnson *et al* (1979)
^{65}Cu	−2·131	Saini *et al* (1983)	^{115}In	−0·293	Hershberger *et al* (1980)
^{67}Zn	−1·783	Johnson *et al* (1960)	^{116}Cd	−1·300	Johnson *et al* (1979)
^{68}Zn	−3·702	Esat *et al* (1981)	^{117}Sn	−2·603	Johnson *et al* (1977)
^{71}Ga	−1·018	Johnson *et al* (1960)	^{119}Sn	−1·361	Johnson *et al* (1977)
^{75}As	−1·647	Johnson *et al* (1960)	^{120}Sn	−3.468	Johnson *et al* (1977)
					Drenckhahn *et al* (1980)
^{77}Se	−2·147	Johnson *et al* (1960)	^{122}Sn	−2·405	Johnson *et al* (1977)
^{80}Se	−2·653	Kailas *et al* (1979)	^{124}Sn	−1·436	Johnson *et al* (1977)
					Drenckhahn *et al* (1980)
^{89}Y	−3·616	Johnson *et al* (1968)	^{128}Te	−2·050	Johnson *et al* (1979)
^{92}Zr	−2·789	Flynn *et al* (1979)	^{130}Te	−1·229	Johnson *et al* (1979)

which is expected to be valid at sub-Coulomb energies and above neutron threshold E_{thr} (500 keV above E_{thr}) and use the fact that

$$\sum_{J_i} (2J_i + 1) = (2J_0 + 1)\,(2j_p + 1),$$

the above expression reduces to

$$\sigma_{p,n} = \pi \lambda\!\!\!^{-2}_p \sum_{j_p, l_p} \frac{(2j_p + 1)}{(2S_p + 1)} T_{l_p j_p}(E_p).$$

Further using the fact $\mathbf{j}_p = \mathbf{l}_p + \mathbf{S}_p$ and $S_p = 1/2$ we get

$$\sigma_{p,n} = \pi \lambda\!\!\!^{-2}_p \sum [(l_p + 1)\, T_{l_p j_p \uparrow} + l_p\, T_{l_p j_p \downarrow}]$$

where $\quad j_{p\uparrow} = l_p + \tfrac{1}{2}; \qquad j_{p\downarrow} = l_p - \tfrac{1}{2}.$

If we further neglect the spin orbit interaction, and use the fact

$$(2l_p + 1)\, T_{l_p} = (l_p + 1)\, T_{l_p j_p \uparrow} + l_p\, T_{l_p j_p \downarrow}$$

we get $\quad \sigma_{p,n} = \pi \lambda\!\!\!^{-2}_p \sum_{l_p} (2l_p + 1)\, T_{l_p}.$

The above expression is identical to the absorption cross-section (σ_{abs}) calculated using the optical model.

In general,

$$\sigma_{p,n} = \sigma_{abs} - \sigma_{CE},$$

and

$$\sigma_{el} = \sigma_{SE} + \sigma_{CE}.$$

where σ_{CE}, σ_{SE} are the compound elastic and the shape elastic cross-sections respectively. Using the optical model we can calculate σ_{SE} and σ_{abs}. Experimentally what we measure are $\sigma_{p,n}$ and σ_{el}. At these low energies in the forward angular region the elastic scattering is dominated by the Coulomb scattering (hence has poor sensitivity to nuclear potential variation) and at backward angles the contributions from compound elastic scattering may be comparable to the shape elastic scattering. Hence the conventional method of determining the optical model parameters through elastic scattering differential cross-section measurement is not suitable at these low proton energies. However, as σ_{CE} is negligible as compared to σ_{abs}, at low proton energies and above the neutron threshold, the optical parameters are best determined by analyzing the $\sigma_{p,n}$ data with the valid assumption $\sigma_{p,n} \sim \sigma_{abs}$ (Johnson *et al* 1977, 1979; Kailas *et al* 1975, 1979) or performing a full Hauser-Feshbach calculation for $\sigma_{p,n}$. There are several instances where $\sigma_{p,p}$ data obtained using both the polarized (Drenckhahn *et al* 1980) and the unpolarized protons (Schrils *et al* 1979) have been used along with the $\sigma_{p,n}$ data to constrain parameters in a better way.

The optical model analysis can be carried out in a fully phenomenological or fully microscopic approach. However, a semi-phenomenological/semi-microscopic approach is sometimes sufficient to bring out the physics involved and at the same time provide the parameters for further calculations. In the present review we have generally followed the phenomenological approach and in §4, the microscopic interpretation of the phenomenological parameter is also considered.

3.2 *Phenomenological analysis*

In the phenomenological approach for determining the optical model parameters one can think of several possibilities:— fit data for a given A_T and E_p (individual), fit data over a small region of A_T and/or E_p range (regional) or fit for a large range of A_T and E_p (global). Each of the above methods has certain merits depending on the interest one has. The first approach gives the best description for a given A_T and E_p and is in general valid for this case only. The regional approach can throw light on the behaviour for a range of E/A with respect to parameter variations. This is suitable for interpolation of parameters in the given range and also to look for special features over a small domain of A/E. The global approach can give the overall behaviour of the parameters with A_T and E_p variations and is more useful for a general understanding in terms of nucleon-nucleus interaction.

In carrying out the phenomenological analysis in this low energy region, the optical model used consisted of a real part which has a Woods-Saxon form and an imaginary part which has conventionally a derivative Woods-Saxon or Gaussian form. (Hodgson 1971). The optical potential at energy E_p is given by

$$V(r, E) = -V_R(E) f_R(r, R_R, a_R) + i 4a_I W_I(E)\, g_I(r, R_I, a_I) + V_c(r, R_c),$$

where V_R = depth of the real potential
W_I = depth of the imaginary potential

$$f_R = 1/(1+\exp[(r-R_R)/a_R])$$

$$g_I = \frac{\mathrm{d}}{\mathrm{d}r}[1/(1+\exp[(r-R_I)/a_I])]$$

$$R_X = R_{0X} A_T^{1/3}$$

R_X = half value radius; a_x = diffuseness parameter

V_C = Coulomb potential taken as potential for a uniformly charged sphere

where

$$V_c = Z_T e^2/r \quad \text{for } r > R_c,$$

and

$$V_c = \frac{Z_T e^2}{2R_c}[3-(r/R_c)^2] \quad \text{for } r \leqslant R_c.$$

In the present discussion we have not included the spin-orbit potential as the calculated σ_{abs} values are rather insensitive to this component of the potential. In principle one can vary all the various parameters associated with the real and the imaginary parts simultaneously and obtain a fit to the data. In this way we will not be able to study the various systematic features associated with the parameters.

Further, as the parameters are correlated it is desirable to keep certain parameters fixed using other criteria and vary only the relevant and the sensitive ones to best fit the data. Following this approach we can hope to learn more about the parameter systematics. Several attempts have been made in the past to look at the correlation of the various parameters in analyzing the $\sigma_{p,n}$ data (Johnson *et al* 1979; Flynn *et al* 1985; Viyogi 1983). Based on these experiences, it is possible to keep the parameters at predetermined values and vary only a few parameters. This is the approach followed by Johnson *et al* (1979) and Kailas *et al* (1979). In the present review we will basically follow the above approach in dealing with the various parameters. It may be mentioned that over the years our knowledge of the microscopic nucleon-nucleus optical model has advanced considerably (Von Geramb 1979, 1985) so it is possible and feasible to make use of certain features of the microscopic result to fix the parameters in carrying out the phenomenological analysis.

In the following sub-sections we deal with each parameter individually and describe in what way its value has been fixed determined from the analysis of (p, n) data.

3.3 *Real potential parameters*

3.3a *Depth*: The real potential as mentioned before is assumed to have a Woods-Saxon form and is taken as local in character. Hence the depth $V_R(E)$ can be expressed as

$$V_R(E) = V_R(0) - V_{\text{EC}} E_p,$$

where V_{EC} is the energy coefficient. To take into account the isoscalar and the isovector components of the proton and the target nucleus interaction explicitly, $V_R(0)$ is

represented as

$$V_{IS}+\frac{N_T-Z_T}{A_T}V_{IV}$$

where V_{IS} is the isoscalar component and V_{IV} is the isovector component. Implicitly we have assumed that energy dependence (if any) of both V_{IS} and V_{IV} has been included in the energy coefficient V_{EC}. Having defined the various terms, we go on to discuss the actual determination of the various components of the parameter V_R.

3.3b *Energy coefficient*: As the nucleon-nucleus optical potential is non-local in character to facilitate the calculation in solving the Schrödinger equation it is the normal practice to use the equivalent local potential. This leads to the energy-dependent term V_{EC} in the real potential. The energy coefficient V_{EC} takes care of not only the non-local to local transformation but also includes the contribution due to the intrinsic energy dependence of the optical potential (Sinha *et al* 1973). From phenomenological analysis spanning a range of proton energies between 3 and 60 MeV, various values of V_{EC} have been obtained. In figure 2, the V_{EC} values of Perey (1963), Becchetti and Greenlees (1969), Menet *et al* (1971) and Johnson and Kernell (1970) have been plotted as a function of E_p-E_F (Fermi energy $E_F=-8$ MeV) values. The horizontal error bars indicate the ranges over which the V_{EC} values have been determined and the V_{EC} values themselves have been plotted at the respective mean E values. An empirical fit to the V_{EC} versus E_p-E_F data yielded

$$V_{EC}=1{\cdot}267\exp[-0{\cdot}0343\,(E_p-E_F)]\quad \text{MeV}.$$

It is thus found that V_{EC} varies rather nonlinearly with E_p. This effect is most pronounced at low energies and this is often referred to as the anomalous variation of the real part (Eck and Thompson 1975; Gyarmati *et al* 1979; Kailas *et al* 1979; Bauer *et al* 1982). Further discussion on this feature will be made in §4. It is enough for the present to note that $V_{EC}\sim 0{\cdot}85$ for $E_p\sim 4$ MeV, roughly the average of the energy range of our interest.

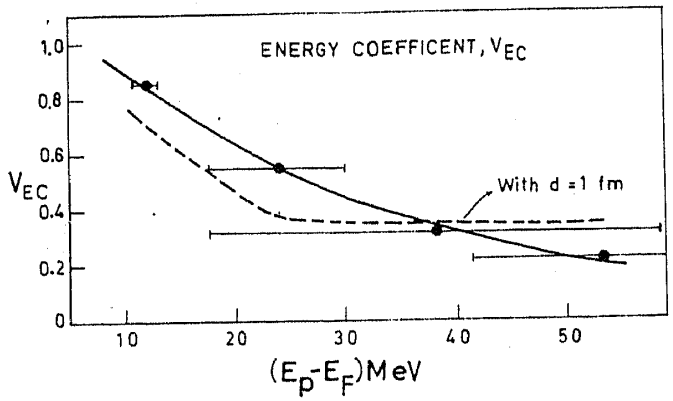

Figure 2. Variation of energy coefficient, V_{EC} as a function of E_p-E_F MeV, with $E_F\sim -8$ MeV. The continuous line is the fit to the V_{EC} data with the expression 1·267 exp $(-0{\cdot}0343\ (E-E_F)$ (MeV)). The dotted line is the calculation with the non-locality parameter, $d\sim 1$ fm.

3.3c *Coulomb correction term*: It is to be remembered that there are differences introduced in the optical potential for the neutrons and the protons due to the Coulomb field of the nucleus. Besides the addition of the trivial Coulomb potential $V_c(R_c)$ for the protons, one also has to use an effective energy $(E_p - \langle V_c \rangle)$ when the proton moves through the Coulomb field of the protons inside the nucleus and $\langle V_c \rangle$, the Coulomb field averaged over the size of the nucleus

$$\left[\langle V_c \rangle = \frac{6}{5} \frac{Z_T e^2}{R_c} \right].$$

In view of this

$$\begin{aligned} V_R(E) &= V_R(0) - V_{EC}(E_p - \langle V_c \rangle) \\ &= V_R(0) - V_{EC} E_p + V_{EC} \langle V_c \rangle \\ &= V_R(0) - V_{EC} E_p + V_{cc} \frac{Z_T}{A_T^{1/3}} \end{aligned}$$

$$\left(V_{cc} = V_{EC} \frac{e^2}{R_0} \frac{6}{5}; \quad R_c = R_0 A_T^{1/3}\right).$$

V_{cc} is the Coulomb correction term. Typically $V_{cc} = 0{\cdot}4$ when $V_{EC} = 0{\cdot}30$ (Perey 1963). Some attempts have been made to determine V_{cc} from the $V_R(E)$ values of the proton and the neutron obtained at the same E ($E = E_p = E_n$) for nuclei ^{40}Ca and ^{28}Si (Rapaport 1982), and determined $V_{cc} = 0{\cdot}5 \pm 0{\cdot}07$. In conventional analysis one normally uses a value of 0·4–0·5 for V_{cc}. The value of $V_{cc} \sim 0{\cdot}5$ obtained by Rapaport is for $E > 10$ MeV. The point to note here is that V_{cc} is dependent on V_{EC} and hence as pointed out §3.3b that if V_{EC} is very large at low energies, V_{cc} will go up proportionately to large values. If $V_{EC} \sim 0{\cdot}85$, $V_{cc} \sim 1{\cdot}1$. So to be consistent with the large value of V_{EC}, in carrying out the analysis at low E_p values one should use a larger value of V_{cc}. Even though Kailas *et al* (1979) used a larger V_{EC} value, they did not use a larger value of V_{cc} in their analysis. Viyogi (1983) used a value of $V_{cc} \sim 1{\cdot}1$ consistent with the value of $V_{EC} \sim 0{\cdot}85$ in reanalyzing the (p, n) data for $A_T = 40$–140.

3.3d *Isoscalar and isovector components*: It is in principle possible to determine isoscalar V_{IS} and isovector V_{IV} components of V_R using the following expression for proton nucleus system,

$$V_R^p = V_{IS} + V_{IV} \frac{N_T - Z_T}{A_T} + V_{cc} \frac{Z_T}{A_T^{1/3}}.$$

If V_R^p is determined for a number of target nuclides specified by Z_T and A_T, the above expression can be used to calculate V_{IS} and V_{IV}. Alternatively this expression can be combined with the expression corresponding to the neutron-nucleus system

$$V_R^n = V_{IS} - V_{IV} \frac{N_T - Z_T}{A_T}$$

for the same target (or targets) and same energy, then we can determine

$$V_{IS} = \tfrac{1}{2}\left[(V_R^p + V_R^n) - V_{cc}\frac{Z_T}{A_T^{1/3}} \right],$$

and

$$V_{IV} = \frac{1}{2\left(\dfrac{N_T - Z_T}{A_T}\right)}\left[(V_R^p - V_R^n) - V_{cc}\frac{Z_T}{A_T^{1/3}} \right].$$

Of course, for the protons one will have to fix the V_{cc} term by the procedure discussed in §3.3c. It can be seen that the latter approach will yield more reliable values of V_{IS} and V_{IV} components, as the $V_R^p - V_R^n$ differences are much larger than the V_R^p changes observed as a function of $(N-Z)/A$ values of the targets.

Viyogi (1983) following the former approach reanalyzed most of the (p, n) data for nuclei lying between $A_T \sim 40$–130, starting with $V_{EC} \sim 0{\cdot}85$ and hence with $V_{cc} \sim 1{\cdot}13$. He has obtained for the various targets (first approach), $V_{IS} \sim 55$ MeV and $V_{IV} \sim 22$ MeV. In the present work we have determined V_{IS} and V_{IV} components by the latter approach and by combining the proton- and the neutron-nucleus parameters of Johnson *et al* (1979) and Smith *et al* (1984) respectively for $A_T \sim 100$. The V_R^n values of Smith *et al* (1984) have been first corrected for the differences in the geometry parameters, R_R, a_R, of Smith *et al* and those of Johnson *et al* as follows:

$$V_R^n = \frac{\left\{ V_R^n R_R^3 \left[1 + \dfrac{\pi^2 a_R^2}{R_R^2} \right] \right\}}{\left\{ R_R^3 \left[1 + \dfrac{\pi^2 a_R^2}{R_R^2} \right] \right\}} \quad \begin{matrix} \text{Smith } et\ al \\ \text{Johnson } et\ al. \end{matrix}$$

In table 2, the V_R^p and the corrected V_R^n values are listed. Combining these two and using the values of $V_{EC} \sim 0{\cdot}32$ and $V_{cc} \sim 0{\cdot}45$ as quoted in the work of Johnson *et al* (1979), we obtain, $V_{IS} \sim 55$ MeV and $V_{IV} \sim 26$ MeV. It must be mentioned that the determination of V_{IS} and V_{IV} strongly depends on the values of V_{cc} which in turn depends on the value of V_{EC}. Using the values of $V_{EC} \sim 0{\cdot}85$, and $V_{cc} \sim 1{\cdot}1$, in the above analysis we get (table 2) $V_{IS} \sim 52$ MeV, $V_{IV} \sim 1$ MeV. It can be seen that the determination of V_{IS} is less sensitive to V_{EC} variations. But the V_{IV} value is drastically affected by the choice of V_{EC}.

Following yet another technique, Flynn (1983) obtained the value of V_{IV} for protons interacting with ^{90}Zr at sub-Coulomb proton energies, from the observed isospin splitting of the $3_{S1/2}$ single-particle resonance. He has described the splitting by the Lane

Table 2. V_{IS} and V_{IV} components of V_R.

A_T	$\dfrac{N-Z}{A}$	V_R^p (MeV)	V_R^n (MeV)	V_{IS} (MeV)	V_{IV} (MeV)	V_{EC} (MeV)
^{89}Y	0·124	62·3	52·9	55	26	0·32
^{93}Nb	0·118	62·3	53·2	52	1	0·85
^{103}Rh	0·126	62·7	50·2			
^{107,109}Ag	0·130	62·9	51·7			
^{115}In	0·148	63·4	50·6			

model with $V_{IV} \sim 31{\cdot}4$ MeV. He has also shown that the V_{IV} determined is strongly dependent on the value of V_{EC} assumed. He gets a value of $V_{IV} \sim 31$ for $V_{EC} \sim 0{\cdot}32$. The values of $V_{IV} \sim 16$ for $V_{EC} \sim 1$ and $V_{IV} \sim 20$ for $V_{EC} \sim 0{\cdot}85$ are also given by Flynn (1983).

A survey of the literature values (Rapaport 1982) of V_{IV} obtained by various methods at slightly higher energies for protons and neutrons, yields an average value around 20 MeV. It may be remarked that the V_{IV} value deduced exclusively from neutron optical model parameters lies between 20 and 30 MeV (Rapaport 1982; Smith *et al* 1984). In this method of determination of V_{IV}, as the V_{cc} term is absent, one does not have the associated uncertainties which generally bother the proton analysis.

Hodgson (1984) detailed the various methods of deducing V_{IV} at higher energies and suggested that the real part can have an A-dependent term and neglect of this will appear as spurious $(N-Z)/A$ dependence. So he suggests that one should have $V_{IV} = V_{IV}^{T} + V_{IV}^{S}$ for protons and $V_{IV} = V_{IV}^{T} - V_{IV}^{S}$ for neutrons where V_{IV}^{T} = true and V_{IV}^{S} = spurious isovector components and by analyzing suitable data it may be possible to separate an A_T dependence from an asymmetry dependence. He has quoted values of $V_{IV}^{T} \sim 21 \pm 3$ MeV and $V_{IV}^{S} = 3 \pm 3$ MeV. As the contribution of the isovector potential to the total potential is small, its determination from phenomenological analyses has a large uncertainty and this will be dependent on how well the total potential is constrained by the analysis.

From the above discussion, it is clear that there are some problems associated with the determination of the V_{IV} component, using the proton data. The V_{IV} values range between 1 and 30 MeV depending on the V_{EC} values. Using exclusively the neutron data, we get V_{IV} values lying between 20 and 30 MeV. The V_{IS} component is perhaps better determined and its values is around $53{\cdot}5 \pm 1{\cdot}5$ MeV.

3.3e *Geometrical parameters for the real potential.* Traditionally one used a Woods-Saxon form for the real part as it is expected to closely follow the nucleon distribution inside the nucleus. A quick look at the literature values of the geometrical parameters of R_{0R} and a_R (Perey 1963; Becchetti and Greenlees 1969; Gianniani and Ricco 1976) reveal they vary between 1·17 and 1·25 fm and 0·57–0·75 fm respectively. Perey (1963) obtained 1·25 fm and 0·65 fm for R_{0R} and a_R respectively. Becchetti and Greenlees (1969) determined R_{0R} and a_R to be 1·17 fm and 0·75 fm respectively. Gianniani and Ricco get 1·25 fm and 0·57 fm respectively for R_{0R} and a_R. In our work carried out at sub-Coulomb energies we have used the values of Becchetti and Greenlees (1969). Giannini and Ricco (1976) showed that in the transformation from non-local to local, besides V, R also becomes energy-dependent. They show that R decreases by 1 fm as E increases from 0 to 60 MeV. For a small energy range with which we are concerned we need not worry about the energy dependence of R.

It has been argued by Finckh (1980) that R need not be always expressed as $R_{0x} A_T^{1/3}$. There can be other dependence on A such as $A_T^{0{\cdot}41}$ instead of $A_T^{1/3}$. He shows that the anomalous variation of V_R with E can be, to a considerable extent, compensated by a proper choice of the A_T dependence of the half-value radius.

It has been argued (Hodgson 1985; Srivastava *et al* 1983) that due to the density dependence of the nucleon-nucleon interaction, R_R and a_R can be expressed as

$$R_R^2 = 1{\cdot}277\, A_T^{2/3} - 3{\cdot}18 + 1{\cdot}24\, A_T^{1/3} - 0{\cdot}38\, A_T^{-1/3}$$

$$\approx 1{\cdot}4\, A_T^{2/3}\ \text{fm}^2 \quad \text{for } A_T > 40,$$

$$a_R^2 = 0{\cdot}53 + 0{\cdot}057\, A_T^{-1/3}$$
$$\approx 0{\cdot}53 \text{ fm}^2 \quad \text{for } A_T > 40.$$

From the above

$$R_{0R} \approx 1{\cdot}18 \text{ fm}; \quad Q_R \approx 0{\cdot}73 \text{ fm}$$
$$(R_R \simeq R_{0R} A_T^{1/3}).$$

These values are very close to the values of Becchetti and Greenlees (1969) and are also the ones we have used in our earlier analysis (Kailas *et al* 1979). However, Johnson *et al* (1979) and Flynn *et al* (1985) use $R_{0R} \sim 1{\cdot}2$ fm and $a_R \sim 0{\cdot}72$ fm. Viyogi (1983) used $R_{0R} \sim 1{\cdot}17$ fm and $a_R \sim 0{\cdot}6$ fm in his global analysis.

3.3f *Summary*: We have summarized in table 3, the real potential parameters, suitable for the sub-Coulomb energy region, obtained by the various groups.

3.4 *Imaginary potential parameters*

At low energies it is conventional to take the imaginary potential to have a derivative Woods-Saxon or Gaussian form, as the absorption is expected to be predominantly in the surface of the nucleus. It is also generally assumed that the imaginary part is local in nature whereas the real part is known to be non-local. For the geometry of the imaginary part, Becchetti and Greenlees (1969) obtained $R_{0I} = 1{\cdot}32$ fm and $a_I = 0{\cdot}51 + 0{\cdot}7\,(N_T - Z_T)/A_T$ fm from their systematic analysis. Kailas *et al* (1979) assumed $R_I = 1{\cdot}32$ fm and $a_I = 0{\cdot}58$ fm in carrying out the analysis of the (p, n) data and searched only on the depth W_I to fit the data. No energy dependence on W_I has been included in this work. Johnson *et al* (1979) kept $R_{0I} = 1{\cdot}3$ fm and searched on W_I and a_I. Again no energy dependence for W_I has been considered. The average value of $a_I \sim 0{\cdot}4$ fm has been obtained by them. Viyogi (1983) from the global analysis gets a value of $a_I = 0{\cdot}84 - 0{\cdot}00265\, A_T$ fm. He used a value of $R_{0I} = 1{\cdot}306$ fm. He also does not include the energy dependence for W_I. Flynn *et al* (1985) get values of R_{0I} and a_I close to those of Johnson *et al* (1979). They have however used energy-dependent W_I and show that W_I

Table 3. Real potential parameters.

	Kailas *et al* (1979) $45 \leqslant A_T \leqslant 80$	Johnson *et al* (1979) $89 \leqslant A_T \leqslant 130$	Viyogi (1983) $40 \leqslant A_T \leqslant 130$
V_{EC} (MeV)	0·85	0·32	0·85
V_{CC} (MeV)	0·40	0·45	1·13
V_{IS} (MeV)	59·2	55·4	55
V_{IV} (MeV)	24	24	22
R_{0R} (fm)	1·17	1·20	1·17
a_R (fm)	0·75	0·73	0·60

$$V_R = V_{IS} + \frac{N_I - Z_T}{A_T} V_{IV} + V_{cc} \frac{Z_T}{A_T^{1/3}} - V_{EC} E_P$$

$$R_R = R_{0R} A_T^{1/3}$$

increases linearly as $W_I \sim W_I(0) + 1{\cdot}7\,E$ MeV. They find that, extrapolation of W_I to higher energies leads to W_I matching with the values determined from analysis at higher energies.

In priniciple, it is possible to express W_I as

$$W_I(E) = W_{IS} + \frac{N_T - Z_T}{A_T} W_{IV} + W_{cc} \frac{Z_T}{A_T^{1/3}} + W_{EC} E_p,$$

where the various terms have meanings similar to those defined for the real part. It has been pointed out by Rapaport (1982) that W_I should include the Coulomb correction term, W_{cc} similar to that found for the real part. However, as W_I increases with increase of energy in contrast to V_R which decreases with increase of energy, the sign of W_{cc} will be opposite to that of V_{cc}. He has determined W_{cc} by combining appropriate proton and neutron optical parameters for ^{40}Ca. His result is

$$W_{cc} = -(1 - 0{\cdot}028\,E_p)\,0{\cdot}5.$$

It can be seen that W_{cc} is energy-dependent and it will vanish for $E \sim 35$ MeV from where W_I becomes almost energy-independent for E_p upto ~ 100 MeV. Viyogi (1983) made an attempt to obtain the W_{cc} from analysis of (p, n) data. However, he has to fix the isovector part of W_I using some other criterion. He finds a value of W_{cc} which is about four times the value quoted above (Rapaport 1982) which is from an analysis at slightly higher E_p values. The situation is less clear as regards the isovector component of the imaginary part, particularly in the low proton energy region.

Without going into further details regarding the various components of W_I, we will go on to discuss the overall behaviour of W_I after fixing R_{0I} and a_I at suitable values. Johnson *et al* (1979) found the W_I values determined from their fits to the (p, n) data varied rather anomalously with A_T for $A_T = 89$–130. (figure 3). Similarly, Kailas *et al* (1979) found that W_I varies anomalously but less strikingly as compared to that of

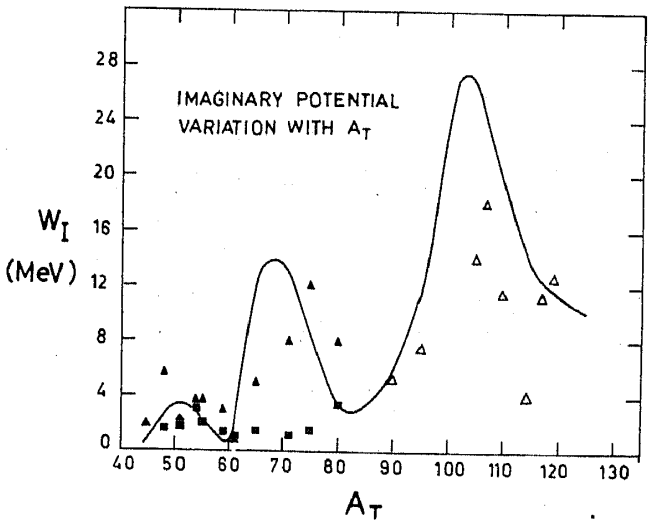

Figure 3. Variation of the imaginary potential W_I with the target mass number A_T. The continuous line is the curve drawn the phenomenological W_I values to guide the eye. The filled squares are calculations based on the relation $W_I \propto [B(E2)]^{\frac{1}{2}}/A_T$. The filled triangles are related to level density of residual nuclei for $E_p \sim 4$ MeV. The open triangles are due to $2p - 1h$ state density calculation of Grimes (1980) (as discussed in the text).

Johnson *et al* (1979) for $A_T = 45$–80, (figure 3). The work of Johnson *et al* (1979) has been extended by the Kentucky Group (Flynn *et al* 1979, 1982, 1985; Hershberger *et al* 1980; Schrils *et al* 1979) who carried out systematic investigation of more nuclei in this mass region and analyzed (p, p) excitation function data along with the (p, n) data. They also confirm the findings of Johnson *et al* (1979). The Erlangen group (Fiegel *et al* 1980, Drenckhahn *et al* 1980) have also looked into some nuclei in this mass region. They combine the (p, p) angular distribution of analyzing power data at selected energies along with the (p, n) excitation function data. They find that the analyzing power data determine only the product $W_I a_I$; however, the (p, n) data do not have this ambiguity. By combining the two kinds of data they are able to determine W_I and a_I individually. They also end up with $a_I \sim 0{\cdot}4$ fm and W_I values for Sn and Ag nuclei consistent with those of Johnson *et al* (1979) and Flynn *et al* (1985).

The main point to note is that the W_I values are in general small as compared to the values obtained at higher energies. Further the W_I values vary rather anomalously with the A_T variation. It has been noted by Viyogi (1983) that if real potential is fixed according to §3.1 and with R_{0I} and a_I given by him, he does not find the anomalous variation of W_I with A_T in the mass region A 89–130 to be as dramatic as found by Johnson *et al* (1979). It is implied that the W_I determination is sensitive to the value of V_R. In §4, we discuss further the anomalous variation of W_I with A_T. In table 4, the W_I values determined by the several groups (Johnson *et al* 1977, 1979; Kailas *et al* 1979; Viyogi 1983) are listed. The corresponding V_R values as mentioned earlier are listed in table 3.

4. Discussion

4.1 *Real potential*

In §3 it was mentioned that the most striking feature of V_R is the observation of the large value of V_{EC} at lower E_p values. It may be pointed out that this anomalous variation of V_R with E near the Fermi energy has been noticed, both for the protons and the neutrons (Finlay *et al* 1985). A few attempts have been made to understand this observation of enhanced V_{EC} values in terms of the effects of non-locality and channel coupling between the incident nucleons and collective states of the target nucleus (Mahaux *et al* 1986, Mahaux and Ngo 1981, 1982, 1983; Hodgson 1984; Gyarmati *et al* 1979, 1981; Eck and Thompson 1975; Kailas *et al* 1979). It may be remarked that for the heavy ions the second order correction to V_R due to the energy dependence of W_I is very significant (Mahaux *et al* 1986) at energies near the Coulomb barrier.

To investigate the effect of the non-local nature of the potential we write following Eck and Thompson (1975)

$$V_{EC}/V_R = \gamma_R,$$

$$\gamma_R = \frac{+1}{\dfrac{V_R}{1+\exp[(r_T - R_R)/a_R]} + \dfrac{2\hbar^2}{md^2}}, \quad E \sim B_c,$$

$$r_R = \frac{1}{V_R + \dfrac{2\hbar^2}{md^2}}, \quad |E - B_c| \gg 0.$$

Table 4. Imaginary potential parameters.

(a) $45 \leqslant A_T \leqslant 80$ Kailas *et al* (1979); $R_{0I} = 1{\cdot}32$ fm; $R_I = R_{0I} A_T^{1/3}$; $a_I = 0{\cdot}58$ fm

A_T	W_I (MeV)	A_T	W_I (MeV)
45	1·4	61	0·4
48	2·2	65	14·3
51	3·7	71	12·4
54	1·9	75	11·5
59	2·2	80	4·0

(b) $89 \leqslant A_T \leqslant 130$ Johnson *et al* 1979; $R_{0I} = 1{\cdot}30$ fm; ($R_I = R_{0I} A_T^{1/3}$. *Johnson *et al* (1977a)

A_T	W_I (MeV)	a_I (fm)	A_T	W_I (MeV)	a_I (fm)
89	5	0·40	113	15·3	0·38
93	6·5	0·40	114	13·7	0·47
103	97	0·39	115	13·9	0·41
105	26·4	0·42	116	11·6	0·41
107	22·5	0·42	122	11·5	0·42*
109	21·3	0·42	124	10·9	0·42*
110	23·4	0·40	128	12·4	0·38
111	18·0	0·40	130	12·3	0·45

(c) $40 \leqslant A_T \leqslant 130$; Viyogi (1983); $R_{0I} = 1{\cdot}306$ fm; $a_I = 0{\cdot}58$ fm.

A_T	W_I (MeV)	A_T	W_I (MeV)
41	1		
45	2		
48	6·8		
49	5	93	6·5
51	6	96	7·5
55	6·5	98	12·2
59	2	103	9
61	1	105	8
65	1.5	107	8·5
68	11·5	109	8·8
71	10·5	110	7
75	10·0	115	6·2
80	13·2	120	7·6
89	2	124	6·5
		128	8·5
		130	7

In the above B_c is the Coulomb barrier height, d, the non-locality parameter and m the nucleon mass. $V_L(r) = V_{NL}(r) \exp - [\frac{1}{2} k(r) d]^2$ is the relation connecting the local V_L and the non-local V_{NL} potential $k(r)$ = local wave number. d is the range of a Gaussian, effective nucleon-nucleon interaction generating $V_N(r)$. r_T = classical turning point for head-on collision:

$$E = \frac{Z_T e^2}{r_T} - \frac{V_R}{1 + \exp[(r_T - R_R)/a_R]}.$$

Using the V_R values given in Perey (1963), Menet *et al* (1971), Becchetti and Greenlees (1969) and Johnson and Kernell (1970) and with $d \sim 1$ fm, V_{EC} values have been computed using the above expressions (figure 2). It can be seen from figure 2 that these values closely reproduce the trend of the V_{EC} values obtained from phenomenological analyses. This analysis shows that the large variation in V_{EC} with E at low energies is a

consequence of using a local potential to approximate a non-local potential and not in disagreement with the values determined at higher energies (Eck and Thompson 1975; Kailas *et al* 1979).

We have also determined the ratio of the effective mass m^* and the nucleon mass m, which will vary with energy as a result of non-locality of the potential. Defining $m^*/m = 1/(1+V_{EC})$ (Eck and Thompson 1975) we find, m^*/m reduces from $\sim 0{\cdot}8$ at $E_p \sim 45$ MeV ($V_{EC} \sim 0{\cdot}22$) to $\sim 0{\cdot}5$ at 4 MeV ($V_{EC} \sim 0{\cdot}85$). These values agree with the findings of Mahaux and Sartor (1986). In addition to the contribution of non-locality to the energy dependence of V_R, we have also investigated the contribution due to the coupling of W_I with V_R. Mahaux *et al* (1986) have given the relation

$$\Delta V_R(E) = \frac{P}{\pi}\int \frac{W_I(E')}{E'-E}\,dE'$$

(P refers to a principal value integral).

As W_I starts increasing at low energies, and reaches a saturation value around 6 MeV (Flynn *et al* 1985) it is expected that the contribution to V_R due to W_I energy dependence is significant at low energies. Using the relation that

$$W_I(E) = \frac{W_0}{(E_b-E_a)}(E-E_a)$$

with $E_a \sim 1$ MeV and $E_b \sim 6$ MeV and $W_0 \sim 12{\cdot}5$ MeV (Flynn *et al* 1985), the second order contribution to V_R (Mahaux *et al* 1986) is

$$\Delta V_R(E) = \left(\frac{W_0}{\pi}\right)(E_a \ln|E_a| - E_b \ln|E_b|)$$

where

$$E_a = \frac{E-E_a}{E_b-E_a} \quad \text{and} \quad E_b = \frac{E-E_b}{E_b-E_a}$$

It works out to a maximum correction of 2·70 MeV and $E \sim 3$ and 4 MeV.

In order to bring out the respective contributions to V_R arising due to the non-locality effect as well as due to energy dependence of W_I, we have made the following analysis: The V_R values obtained at several energies (Johnson and Kernel 1970; Perey 1963; Becchetti and Greenlees 1969; Menet *et al* 1971) have been converted to equivalent V_R, V_R^{EQ} using the relation

$$V_R^{EQ} = \frac{\left\{V_R R_R^3\left[1+\frac{\pi^2 a_R^2}{R_R^2}\right]\right\}}{R_{EQ}^3\left[1+\frac{\pi^2 a_{EQ}^2}{R_{EQ}^2}\right]},$$

with $R_{EQ} = 1{\cdot}17\,A^{1/3}$ fm and $a_{EQ} = 0{\cdot}75$ fm. These values are plotted in figure 4 as a function of E_p values. In the same figure the $\Delta V_R(E)$ values obtained between $1 \lesssim E_p \lesssim 6$ according to the dispersion relation are also plotted. As the correction to V_R from the energy dependence of W_I vanishes beyond $E_p \sim 6$ MeV, it is safe to assume that the energy dependence of V_R for $E_p \geqslant 10$ to 60 MeV is entirely due to the non-

locality effect. With this assumption the V_R values at the average values of $E_p \sim 16$, 30 and 45 MeV, have been fitted with an expression

$$V_R \sim 65 \exp[-0{\cdot}385\,(E_p - E_F)].$$

This is shown as the continuous curve in figure 4. The V_R values obtained from an extrapolation of the above expression to low energies are supposed to represent the contribution due to the non-locality effect. The change in V_R with E_p works out to $\sim$ 0·8 to 0·9 MeV per MeV change of E_p. It is seen from the figure that the continuous curve solely due to the non-locality effect, can reproduce the phenomenological data in the low energy region very well. This agreement can be considered accidental as it has already been shown that the contribution due to coupling effect is significant at low energies. To conclude, we can say that for low energies, both the above mentioned effects need to be considered and it is not possible to estimate reliably their respective contributions from the present work.

4.2 *The imaginary potential*

The most striking feature of the analysis has been the observation of the anomalous variation of W_I with A_T. From figure 3 it can be seen that W_I goes through maxima for A_T values 52, 67 and 103 and minima for $A_T \sim 42$, 61, 84 and 120. In order to see whether these values follow any systematic pattern we have plotted in figure 5 the maxima (minima) number against $A_T^{1/3}$. It is found that the maxima and minima data can be respectively fitted with the expressions

$$n_{\max} = 2{\cdot}04\, A_T^{1/3} - 5{\cdot}49,$$
$$n_{\min} = 2{\cdot}04\, A_T^{1/3} - 6{\cdot}06.$$

This behaviour perhaps indicates the presence of some kind of shell or size effect. The minima around $A_T \sim 42$, 61, 84 and 120 would be due to proton shell (sub-shell) closures for $Z_T \sim 20$, 28, 40 and 50.

Various other explanations have been proposed to understand the observed behaviour of W_I. It has been shown (Hjorth *et al* 1968) that W_I and the $B(E2)$ values are related as

$$J_w/A = x + y\frac{[B(E2)]^{1/2}}{A_T},$$

where J_w/A = volume integral of

$$W_I\left(= \frac{16\pi R_I^2 a_I W_I}{A_T}\left[1 + \frac{\pi^2 a_I^2}{3R_I^2}\right]\right)$$

and x and y are constants. $B(E2)$ connects the first excited state and ground state involving a l change of 2. The $B(E2)$ values have been taken from the nuclear data sheets for the various nuclei. For protons we have shown that except for Cu, Ga and AS—the anomalously behaving nuclides—the average increase of W_I with A_T is explainable in terms of the relationship mentioned above (figure 3). This is an interesting result as it shows that the absorption per unit size (J_w/A) is proportional to the softness of the core and hence brings the connection between the imaginary potential and nuclear structure

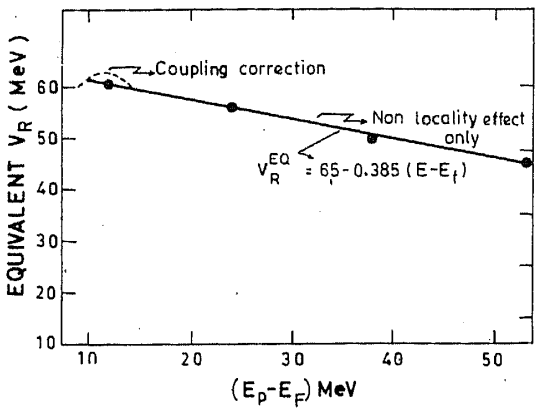

Figure 4. Equivalent potential V_R^{EQ} plotted as a function of $E_p - E_F$ MeV ($E_F \sim -8$ MeV). The straight line is the fit to the data with the expression $V_R^{EQ} = 65 - 0{\cdot}385 \times (E - E_F)$ MeV for $E - E_F > 20$ MeV. The dashed curve is the second order contribution to the real part due to the energy dependence of W_l, calculated as discussed in the text.

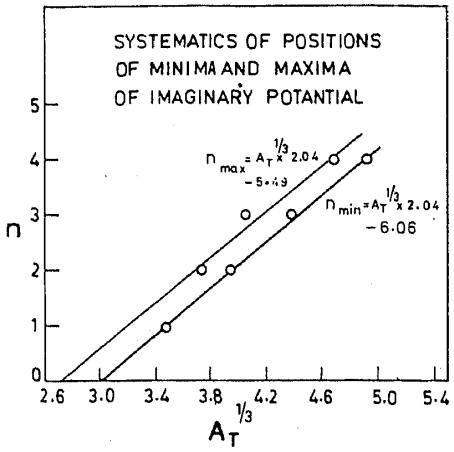

Figure 5. Positions (or the number) of the maxima (minima) of W_l as a function of $A_T^{1/3}$ ($= R$). The straight lines are the fits to the data.

of target nucleus. Another interesting possibility is to look for the correlation between the level density of the proton plus target systems (Grimes 1980) and for the residual nuclei (Kailas *et al* 1979). In figure 3 we have shown these correlations also, where W_l values are suitably normalized to the level density. Grimes (1980) pointed out that the $2p$–$1h$ state densities are the ones to be used and not the actual level densities. It may be pointed out that for neutrons also, Smith *et al* (1984) found anomalous variation in the mass number range $A_T \sim 89$–130. Hodgson (1985) has shown that the level density explanation works well here also. Grimes (1980) also showed that the variation of W_l with A_T in terms of $2p$-$1h$ state density is pronounced at $E_p \sim 3$ MeV and is less prominent at a higher proton bombarding energy of 6 MeV. This prediction is confirmed in the recent phenomenological analyses of Flynn *et al* (1985) who used energy-dependent W_l. At higher energies above the Coulomb barrier the anomalous variation of W_l is totally absent (Careda *et al* 1982). It can be concluded that W_l is sensitive to nuclear structure effects and this effect is most pronounced at low energies and becomes progressively less pronounced at high energies. To sum up the variation of W_l with A_T is dependent on the shell structure of the nuclei, the deformation of the target nuclei and the coupling to the collective states.

4.3 *Strength function analysis*

In order to show not only the goodness of the fitting procedure followed but also to bring out any possible nuclear size effects, strength functions are generally calculated. (Schiffer and Lee 1958; Johnson *et al* 1977, 1979; Kailas *et al* 1979; Flynn *et al* 1985; Bilpuch *et al* 1976; Matsuzaki and Arai 1983). The proton strength function at energy E_p is defined as

$$S_p \simeq S_{p,n} = \frac{\sigma_{p,n}\, R}{4\pi^2 k^{-2} \sum (2l+1)\, P_l}$$

where P_l is the Coulomb penetration factor for protons calculated at $R \sim 1{\cdot}45\, A_T^{1/3}$. The average strength functions (SFN) for the various nuclei from their respective excitation functions are plotted in figure 6 for $E_p \sim 4$ MeV as a function of A_T. In this figure the proton strength function values obtained by Schiffer and Lee (1958) have also been included. It is interesting to note that the curve goes through maxima for $A_T \sim 51$, 68 and 103 similar to the observation for W_l versus A_T curve. The maxima observed for $A_T \sim 51$ and 68 may correspond to the d wave and s wave size resonances predicted by Schiffer and Lee (1958). According to Johnson *et al* for $E_p \sim 6$ MeV, p wave resonance is observed for Sn isotopes. As the contribution of the various l values changes with E_p and A_T, it is possible that we get a peak around $A_T \sim 103$, though less prominent, and it might be due to the p wave size resonance. As noted above the behaviour of SFN with A_T is very similar in character to the variation of W_l with A_T (figure 3).

It is not clear whether there is any direct connection between these two observations. The size resonances are generally characterized by three quantities, the energy of the maximum, the absolute value of reduced cross-section (strength function) and the width of the resonance. The position of the maximum mainly depends on the real potential, the absolute cross-section and the width on the imaginary potential. As W_l and V_R and hence the position of size resonances are related through the transmission coefficient (Preston 1965) it is possible in certain favourable situations, that W_l and strength function exhibit similar behaviour with respect to A_T variation. This point needs to be explored further.

4.4 *Microscopic optical model*

As considerable development has taken place in the microscopic approach to the determination of the optical potential at low energies (Jeukenne *et al* 1977; Lejeune 1980; Giannini and Ricco 1976) it will be interesting to compare the phenomenological values discussed here with the microscopic predictions. In general, the phenomenological real potentials agree with the microscopic values and there are noticeable differences for the imaginary part (Kailas *et al* 1979). It has been found that at higher energies the microscopic imaginary potentials require an overall normalization of the

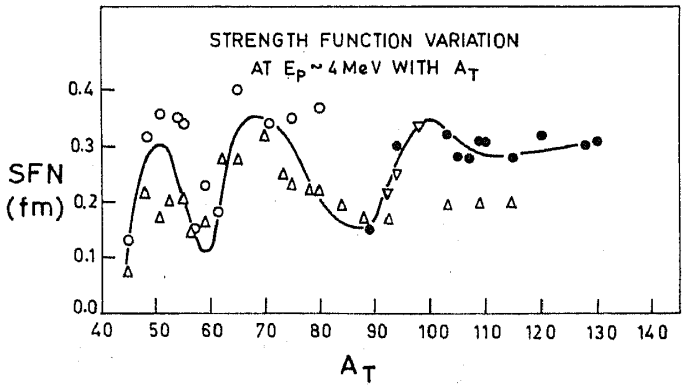

Figure 6. Strength function (SFN) plotted as a function of the target mass number A_T, for $E_p \sim 4$ MeV. The open triangles are from Schiffer and Lee (1958). Their original values have been divided by a factor of two to be consistent with the present definition of strength function. The open circles are from Kailas *et al* (1979). The filled circles are from Johnson *et al* (1979). The inverted triangles are from Flynn *et al* (1985). The continuous line is drawn to guide the eye.

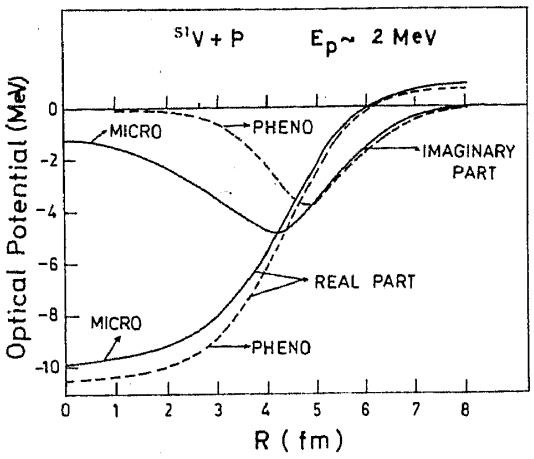

Fig. 7. Comparison of the microscopic and the phenomenological potentials for $^{51}V + p$ system at $E_p \sim 2$ MeV.

order 0·6 to 0·8, to bring them into agreement with the phenomenological values (Lejeune and Hodgson 1978; Bhattacharya and Kailas 1983). The proton absorption cross-sections have also been calculated using the microscopic potentials. At sub-Coulomb energies, these cross-sections closely reproduce the experimental data (Kailas *et al* 1982).

In the present work, we have computed the microscopic optical potentials at $E_p \sim 2$ MeV for $^{51}V + p$ system following Lejeune's (1980) prescription and compared them with the phenomenological values (Kailas *et al* 1979). In figure 7 we have plotted $V_R + V_c$ for the microscopic and the phenomenological cases for $^{51}V + p$ system. In the whole interaction region the two potentials agree fairly well.

We have also plotted in figure 7 the respective imaginary potentials. Here the agreement is not as good as that found for the real part. The maxima and their positions in the two cases do not agree. However the agreement is better for $R > 5$ fm. As pointed out earlier the imaginary part requires normalization. In any case, the microscopic model cannot reproduce the anomalous variation of the imaginary potential W_I with A_T, as it is due to the nuclear structure effect which is not included in the present microscopic calculation.

5. Conclusions

In the present work we have reviewed certain interesting features of low energy (which in the case of protons becomes sub-Coulomb) optical model analysis. It turns out that one should be cautious in extrapolation of parameters determined from analysis at high energies and also interpolation of parameters between A_T values as some of the parameters are known to behave rather anomalously with respect to E and A_T variations. We have brought out the fact that the energy dependence of the real part is in part due to non-locality effect and in part due to coupling to collective states (energy dependence of W_I). However, from the present work, it has not been possible to determine unambiguously their respective contributions in the low energy region. It has been shown that W_I variation with A_T can be understood in terms of mainly the nuclear structure effects which dominate at low energies and become progressively less important at higher energies. A comparison with the microscopic model reveals that the real potential is in good agreement with the phenomenological value but the imaginary

potential requires normalization. To constrain the uncertainties in the parameters determined for $A_T < 89$, more extensive and accurate measurements are necessary. Most of the analysis for this A_T region have been done with the assumption $\sigma_{abs} \sim \sigma_{p,n}$ and hence detailed Hauser-Feshbach analysis will have to be carried out to make sure the variation of parameters like W versus A is due to genuine effects and not due to improper treatment of data. Even in the mass region between $89 \leqslant A_T \leqslant 130$, (p, p) measurements for nuclei like ^{103}Rh are desirable to constrain the imaginary potential parameters in a better way.

Acknowledgements

We are thankful to several of our colleagues (whose names appear in the list of references) for their active participation which contributed to the success of the "(p, n) programme" at Trombay. Special thanks are due to Dr S K Gupta for his valuable suggestions, innovative ideas and keen interest at various stages of this work. We thank Dr Y P Viyogi for his valuable contributions to this programme and for making available to us prior to publication, his results of the exhaustive optical model analysis.

References

Avrigeanu M, Ivascu M and Avrigeanu V 1986 Specialist' meeting on the use of the optical model for the calculation of neutron cross sections below 20 MeV, Paris, NEANDC **222** 279

Bauer M, Hernandez Saldana E, Hodgson P E and Quintanilla J 1982 *J. Phys.* **G8** 525

Becchetti F D and Greenlees G W 1969 *Phys. Rev.* **182** 1190

Bhattacharya S ad Kailas S 1983 *Z. Phys.* **A312** 99

Bilpuch E G, Lane A M, Mitchell G E and Moses J D 1976 *Phys. Rep.* **C28** 145

Careda E, Pignanelli M, Micheletti S, Von Geramb H V, Harakeh M N, De Leo R, D'Erasmo G and Pantaleo A 1982 *Phys. Rev.* **C26** 1941

Drenckhahn W, Feigel A, Finckh E, Gademann G, Ruskamp K, Wangler M and Zemlo L 1980 *Nucl. Phys.* **A339** 13

Eck J S and Thompson W J 1975 *Nucl. Phys.* **A237** 83

Esat M J, Spear R H, Zyskind J L, Shapiro M H, Fowler W A and Davidson J M 1981 *Phys. Rev.* **C23** 1822

Feshbach H, Porter C E and Weisskopf V F 1954 *Phys. Rev.* **96** 448

Feigel A, Finckh E, Ruskamp K and Weise U 1980 *Phys. Rev.* **C21** 2666

Finckh E 1980 *Nukleonika* **25** 1971

Finlay R W, Annand J R M, Pelter J S and Dietrich F S 1985 *Phys. Lett.* **B155** 313

Flynn D S 1983 *Phys. Rev.* **C27** 2381

Flynn D S, Hershberger R L and Gabbard F 1979 *Phys. Rev.* **C20** 1700

Flynn D S, Hershberger R L and Gabbard F 1982 *Phys. Rev.* **C26** 1744

Flynn D S, Hershberger R L and Gabbard F 1985 *Phys. Rev.* **C31** 87

Gabbard F 1977 National Bureau of Standards Spl. Publication 493

Giannini M M and Ricco G 1976 *Ann. Phys.* **102** 458

Grimes S M 1980 *Phys. Rev.* **C22** 436

Gulzar Singh, Kailas S, Saini S, Chatterjee A, Balakrishnan M and Mehta M K 1982 *Pramana (J. Phys.)* **19** 565

Gupta S K and Kerekatte S S 1971 BARC Report No. 579

Gyarmati B, Vertae T, Zolnai L, Baryshnikov A I, Gurbich A F, Titarenko N N and Yadrovsky E L 1979 *J. Phys.* **G5** 1225

Gyarmati B, Lovas R G, Vertse T and Hodgson P E 1981 *J. Phys.* **G7** L209

Hauser W and Geshbach H 1952 *Phys. Rev.* **87** 366

Hershberger R L, Flynn D S, Gabbard F and Johnson C H 1980 *Phys. Rev.* **C21** 896

Hjorth S A, Lin E K and Johnson A 1968 *Nucl. Phys.* **A116** 1
Hodgson P E 1971 *Nuclear reactions and nuclear structure* (Oxford: Clarendon Press) Ch. 5–10.
Hodgson P E 1984 *Rep. Prog. Phys.* **47** 613
Hodgson P E 1985 American Institute of Physics Conf. Proc. No. 124, p. 1
Iyengar K V K 1967 *Nucl. Phys.* **A96** 521
Jeukenne J P, Lejeune A and Mahaux C 1977 *Phys. Rev.* **C16** 639
Johnson C H and Kernell R L 1970 *Phys. Rev.* **C2** 639
Johnson C H, Galonsky A and Inskeep C N 1960 ORNL 2910
Johnson C H, Kernell R L and Ramavataram S 1968 *Nucl. Phys.* **A107** 21
Johnson C H, Bair J K, Jones C M, Penny S K and Smith D W 1977a *Phys. Rev.* **C15** 196
Johnson C H, Galonsky A and Kernell R L 1977b *Phys. Rev. Lett.* **39** 1604
Johnson C H, Galonsky A and Kernell R L 1979 *Phys. Rev.* **C20** 2052
Kailas S, Gupta S K, Mehta M K, Kerekette S S, Namjoshi L V, Ganguly N K and Chintalapudi S 1975 *Phys. Rev.* **C12** 1789
Kailas S *et al* 1979 *Nucl. Phys.* **A315** 157
Kailas S, Gupta S K, Kerekatte S S and Fernandes C V 1985 *Pramana J. Phys.* **24** 629
Kailas S, Mehta M K, Gupta S K, Viyogi Y P and Ganguly N K 1979 *Phys. Rev.* **C20** 1272
Kailas S and Mehta M K 1982 *Proc. of the second Indo-US symposium* (ed.) on *Nucl. Phys. at cyclotron and Intermediate energy* B Sinha p. 505
Kailas S, Gupta S K, Mehta M K and Gulzar Singh 1982b *Phys. Rev.* **C26** 830
Kennett S R 1980a *Nucl. Phys.* **A344** 351
Kennett S R *et al* 1980b *Nucl. Phys.* **A346** 523
Lejeune A and Hodgson P E 1978 *Nucl. Phys.* **A295** 301
Lejeune A 1980 *Phys. Rev.* **C21** 1107
Macklin R L 1957 *Nucl. Instrum. Methods* **1** 335
Macklin R L, Glass F M, Halperin J, Roseberry R T, Schmitt H W, Stoughton R W and Tobias M 1972 *Nucl. Instrum. Methods* **102** 181
Mahaux C and Ngo H 1981 *Phys. Lett.* **B100** 285
Mahaux C and Nago H 1982 *Nucl. Phys.* **A378** 205
Mahaux C and Ngo H 1983 *Phys. Lett.* **B126** 1
Mahaux C, Ngo H and Satchler G R 1986 *Nucl. Phys.* **A449** 354
Mahaux C and Sartor R 1986 *Nucl. Phys.* **A451** 441
Matsuzaki T and Arai E 1983 *Z. Phys.* **A313** 293
Menet J J H, Gross E E, Malanify J J and Zucker A 1971 *Phys. Rev.* **C4** 1114
Perey F G 1963 *Phys. Rev.* **131** 745
Preston M A 1965 *Physics of the nucleus* (New York: Addison-Wesley) p. 519
Rapaport J 1982 *Phys. Rep.* **C87** 25
Sargood D G 1982 *Phys. Rep.* **C93** 61
Saini S *et al* 1983 *Nucl. Phys.* **A405** 55
Satchler G R and Love W G 1979 *Phys. Rep.* **C55** 184
Schiffer J P and Lee L L 1958 *Phys. Rev.* **109** 2098
Schrils R, Flynn D S, Hershberger R L and Gabbard F 1979 *Phys. Rev.* **C20** 1706
Schwandt P 1983 American Institute of Physics Conf. Proc. No. 97 p. 89
Sekharan K K 1966 M.Sc. (Thesis) Bombay University
Sekharan K K, Laumer H, Kern B D and Gabbard F 1976 *Nucl. Instrum. Methods* **133** 253
Sinha B, Srivastava D K and Ganguly N K 1973 *Phys. Lett.* **B43** 113
Smith A B, Guenther P T and Whalen J F 1984 *Nucl. Phys.* **A415** 1
Smith A B, Lewson R D and Guenther P T 1986 Specialists meeting on the use of the optical model for the calculation of neutron cross sections below 20 MeV, Paris, NEANDC **222** p. 183
Srivastava D K, Basu D N and Ganguly N K 1983 *Phys. Lett.* **B124** 6
Viyogi Y P *et al* 1978 *Phys. Rev.* **C18** 1178
Viyogi Y P 1983 Ph.D. (Thesis) Calcutta University
Von Geramb H V 1979 Microscopic optical potentials; *Lecture notes in physics* (Berlin: Springer) Vol. 89
Von Geramb H V 1985 American Institute of Physics Conf. Proc. **124** p. 14
Walter R L and Guss P P 1985 *Proc. Int. Conf. Data for basic and applied science, Santa Fe*, New Mexico, USA
Zyskind J L, Barnes C A, Davidson J M, Fowler W A, Marrs R E and Shapiro M H 1980 *Nucl. Phys.* **A343** 295